The Canadian Mineralogist
Vol. 33, pp. 547-558 (1995)

THE GEOCHEMISTRY OF PHLOGOPITE AND CHLORITE FROM THE KIPUSHI Zn–Pb–Cu DEPOSIT, SHABA, ZAIRE

MUMBA CHABU

Laboratoire de Métallogénie, Université de Lubumbashi, B.P. 1825, Lubumbashi, Zaïre

ABSTRACT

Phlogopite and chlorite have been found in the Kipushi Zn–Pb–Cu deposit, which is hosted by Lower Kundelungu dolomite and dolomitic shale of Late Proterozoic age, and by karstic chimneys and solution-collapse breccias. Electron-microprobe analyses of these minerals indicate that the highest fluorine contents, ranging from 4.41 to 6.39 wt.%, are found in ore-related phlogopite, which also is the most magnesian (X_{Mg} may exceed 0.99) [X_{Mg}: Mg/(Mg + Fe)] and the closest to the phlogopite end-member [X_{phl} (Mg/total octahedral cations) up to 0.95]. These F contents are compatible with the Fe–F avoidance rule and with a disordered distribution of atoms on the octahedral and OH–F sites. In general, X_{phl}, F and Si vary sympathetically, whereas X_{phl} and ^{VI}Al are negatively correlated. Chlorite exhibits a very low F content (0 – 0.73 wt.%) and a considerable spread in composition, with X_{Mg} values ranging from 0.32 to 0.84. The more Fe-rich chlorite is associated with Fe-rich sphalerite (up to 7.86 mol % FeS) as the dominant sulfide. Chlorite in association with chalcopyrite ores has X_{Mg} values around 0.76. The most magnesian chlorite ($X_{Mg} \approx 0.83$) occurs in barren shale of the "Série récurrente", above the mineralization. Calculations of $\log[f(H_2O)/f(HF)]$ based on calibrated F–OH exchange relations between fluid and biotite indicate higher relative activity of fluorine in mineralized areas than in barren rocks. Phlogopite and chlorite are considered to be of metamorphic origin; their composition is interpreted in terms of 1) increasing $f(F)$ and $f(S_2)$ as the orebody is approached, and 2) changes in bulk composition. The emplacement of the orebody probably predated the peak of the Lufilian (Katangan) Pan-African orogeny (650–500 Ma).

Keywords: Kipushi Zn–Pb–Cu deposit, Katangan, Lower Kundelungu Group, phlogopite, chlorite, X_{Mg}, F–OH exchange, Lufilian orogeny, Zaire.

SOMMAIRE

La phlogopite et la chlorite se rencontrent tant dans les minerais que dans les roches encaissantes du gisement Zn–Pb–Cu de Kipushi, localisé dans les dolomies et les shales dolomitiques, en partie bréchifiés, du groupe du Kundelungu inférieur, d'âge protérozoïque supérieur. D'après les données obtenues à la microsonde électronique, les teneurs les plus élevées en fluor, variant entre 4.41 et 6.39%, en poids, se rencontrent dans la phlogopite associée aux minerais; on y trouve également les plus fortes valeurs de X_{Mg} [X_{Mg} = Mg/(Mg+Fe)], dépassant même 0.99, et de la proportion du pôle phlogopite (X_{phl} = Mg/total des cations en sites octahédriques), jusqu'à 0.95. De manière générale, X_{phl}, Si et F varient proportionnellement. En revanche, X_{phl} et ^{VI}Al présentent une corrélation négative. La chlorite est très pauvre en fluor (0–0.73%, en poids). Elle montre par ailleurs d'importantes variations de composition (X_{Mg} de 0.32 à 0.84). Les compositions de chlorite les plus ferrifères sont associées aux minerais à sphalérite ferrifère (environ 7.86%, teneur molaire de FeS) dominante. Dans les minerais à chalcopyrite dominante, la chlorite présente un X_{Mg} d'environ 0.76. La chlorite la plus magnésienne (X_{Mg} = 0.83 en moyenne) caractérise les shales dolomitiques de la Série récurrente, stratigraphiquement au-dessus de la minéralisation. Les calculs de $\log[(f(H_2O)/f(HF)]$ fondés sur les relations d'échange F–OH entre fluide et biotite indiquent une activité relative de fluor plus élevée dans les minerais que dans l'encaissant. La phlogopite et la chlorite seraient d'origine métamorphique. Leur composition reflèterait l'augmentation de $f(F)$ et de $f(S_2)$ vers le gisement et la composition globale des roches. Le gisement aurait été formé antérieurement au paroxysme de la tectonique lufilienne (650–500 Ma).

Mots-clés: gisement Pb–Zn–Cu de Kipushi, Katanguien, Kundelungu inférieur, phlogopite, chlorite, X_{Mg}, échange F–OH, minéraux métamorphiques, orogenèse lufilienne, Zaïre.

INTRODUCTION

The origin of the Kipushi deposit is controversial. Intiomale & Oosterbosch (1974) and Intiomale (1982) considered ascending hydrothermal solutions of magmatic origin as progenitors of the mineralization. De Magnée & François (1988) related the Kipushi deposit to the dissolution of a salt diapir, which produced the breccia in the anticlinal core. The resulting brines are taken to be the mineralizing fluids, and the mineralization is considered to be postkinematic. The deposit has also been ascribed to deposition from fluids

formed by metamorphic dewatering (Unrug 1988). Chabu (1990) and Chabu & Boulègue (1992) suggested that the mineralized solution-cavities are karstic features, and considered the formation of karst and the main part of the mineralization to be contemporaneous and to predate the peak of the Lufilian tectonism. Mineral compositions presented in this paper support this hypothesis.

Many thermodynamic variables can influence the complex geochemistry of a trioctahedral mica and of a chlorite; their composition may be employed to estimate some of the physicochemical conditions associated with their crystallization. In particular, as a result of the experimental work of Munoz & Ludington (1974, 1977) and Zhu & Sverjensky (1992), the F content of micas has been used to gain information about the nature of the fluid phase during metamorphism and ore deposition.

In this study, we provide analytical data on the F:OH ratio of phlogopite in a sediment-hosted base-metal deposit; trends of compositional variables of both phlogopite and chlorite place constraints on genetic models.

Geological Setting

The Kipushi Zn–Pb–Cu deposit is one of the major producers of zinc, cadmium and germanium in Africa. It is located about 30 km west-southwest of Lubumbashi, in southeastern Zaire, on the Lufilian tectonic arc (Fig. 1). The deposit lies along the eastern margin of a body of collapse breccia that occupies the axial portion of the Kipushi anticline and discordantly transects the strata of the northen flank of the anticline (Fig. 2).

The Lufilian tectonic arc, also known as the Copperbelt owing to its considerable copper reserves and production figures, consists of nearly 10,000 m of Late Proterozoic Katangan strata. These are subdivided into the Roan and Kundelungu supergroups (Table 1). The latter consists of two subunits, the Lower and the Upper Kundelungu groups. The base of both the Lower

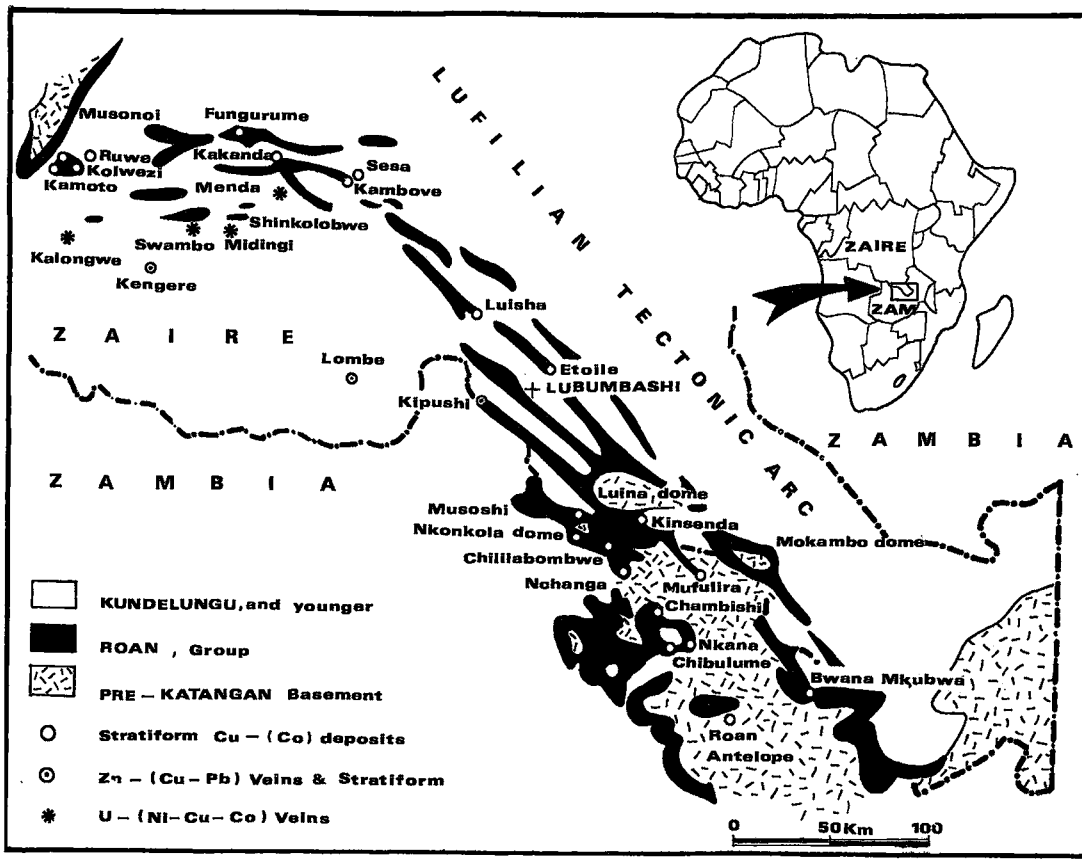

FIG. 1. Simplified geology of the Lufilian fold belt, showing the locations of major Copperbelt deposits. Modified after Sodimiza mining company records, Chabu & Boulègue (1992).

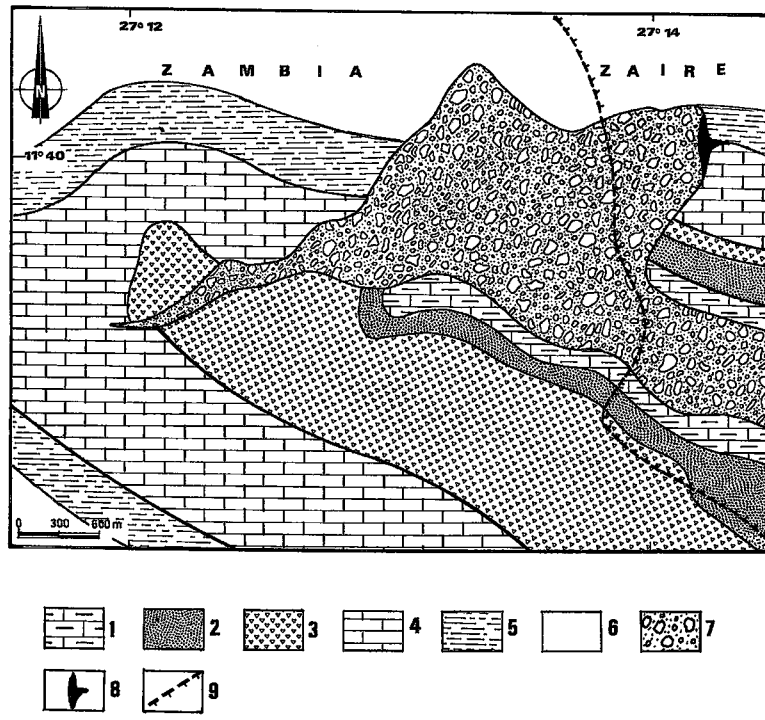

FIG. 2. Geological map of the center of the Kipushi anticline and location of the deposit. Modified after Intiomale (1982) and Chabu & Boulègue (1992). Symbols: 1 siliceous dolomite (Lower Mwashya, 2 shale (Upper Mwashya), 3 Grand Conglomérat, 4 dolomite (Kakontwe), 5 shale and dolomite (Série récurrente), 6 shales and sandstones, 7 breccia, 8 ore deposit, 9 international boundary.

Kundelungu and the Upper Kundelungu groups is placed at the lithostratigraphic markers called the "Grand Conglomérat" and the "Petit Conglomérat", respectively. Both units have a tillitic origin (Intiomale 1982). On the Zairean segment of the Lufilian tectonic arc, the Katangan rocks have been subjected to low-grade metamorphism during the Katangan orogeny (*ca.* 650–500 Ma).

In the axial zone of the Kipushi anticline, the breccia body is composed of very large blocks (up to more than a hundred meters across) of Roan rocks of different lithologies. Among them are fragments of white sparry dolomite assigned to Dipeta Group (Lefebvre 1975), and arkosic sandstone. Blocks of gabbro have also been found in the breccia. These represent a sill-like intrusion of gabbroic rocks, now completely amphibolitized, probably emplaced in the Dipeta dolomite (Lefebvre 1975).

At its eastern margin, the breccia body is composed of rock fragments derived from the enclosing Lower Kundelungu beds. The unit has been interpreted as a collapse breccia (De Magnée & François 1988, Chabu 1990, Chabu & Boulègue 1992) probably emplaced before the peak of the Lufilian (Katangan) orogeny (*ca.* 650–500 Ma) and will be referred to as the Kipushi breccia.

As shown in Figure 2, the polymetallic mineralization of the Kipushi deposit is located in Lower Kundelungu Group rocks at the base of the "Série récurrente", a sequence of alternating dolomite and shale, and in the underlying Kakontwe dolomite, where it is confined to stratabound and discordant paleokarst structures. It also occurs in the Kipushi breccia. The mineralized breccia is limited toward the west between levels –160 and –1800 m by a large barren block composed of shale and fine dolomitic sandstone. It has been termed the "Grand lambeau" and considered to belong to the Upper Kundelungu Group by Intiomale (1982). The sulfides in the deposit, in order of abundance, are sphalerite, chalcopyrite, bornite, pyrite, chalcocite, arsenopyrite, tennantite, galena, renierite with minor briartite, gallite, germanite, carrolite, betechtinite, molybdenite and stromeyerite (Intiomale 1982, Chabu 1990). They form three ore types: (i) copper ores mostly located in the "Série récurrente", (ii) mixed ores (Zn + Pb + Cu) hosted by Upper

TABLE 1. SCHEMATIC STRATIGRAPHIC COLUMN OF THE KATANGAN SEDIMENTARY SEQUENCE ON THE ZAIREAN COPPERBELT, SOUTHEASTERN SHABA, ZAIRE

	SUPERGROUP	GROUP	FORMATION	LITHOLOGY
KATANGAN SEQUENCE	Kundelungu	Upper		shale and sandtone
				shale
			Petit Conglomérat	tillite
		Lower		shale
			Série récurrente	dolomite and shale
			Kakontwe	dolomite and shale
			Kaponda	dolomite and shale
			Grand Conglomérat	tillite
	Roan	Mwashya		sandstone, shale and dolomite
		Dipeta		dolomite, shale and sandstone
		Mines		shale, dolomite and sandstone
		R.A.T.		shale and sandstone
Kibara Supergroup and older rocks (Basement complex)				

The base of the R.A.T. Group is unknown in this area. The three basal Roan Groups invariably appear as slabs of variable size, up to several km across, in megabreccias. R.A.T.: roches argilo-talqueuses (argilaceous talc-bearing rocks; actually, fine-grained sandstone). Modified after Chabu & Boulègue (1992).

Kakontwe dolomite, and (iii) zinc ores mainly located in Middle and Lower Kakontwe dolomite as discordant karstic pipe-fillings surrounded by pyritic ores. The three types of ore are present in the Kipushi breccia.

Fe sulfides in ores are represented by chalcopyrite, pyrite, arsenopyrite and minor marcasite. Arsenopyrite is commonly associated with Cu sulfides, mainly chalcopyrite, and with pyrite in pyritic ores. No pyrrhotite was found in this study, but Intiomale & Oosterbosch (1974) reported blebs of this mineral in some grains of chalcopyite. In general, the assemblages of ore minerals indicate a sulfur fugacity too high to allow the formation of pyrrhotite at this grade of metamorphism (see below).

Widespread structural and textural features indicate that the deposit predates the peak of the Katangan deformational event. These include the presence of folded, sheared and brecciated ores (Chabu 1990, Chabu & Boulègue 1992).

Sampling and Petrographic Observations

Phlogopite- and chlorite-bearing samples have been observed both in barren and mineralized environments (Appendix 1). Those from barren zones occur in shale and dolomite of the "Série récurrente" above the mineralization and in gabbro blocks of the Kipushi breccia body sampled in drill cores. Phlogopite- and chlorite-bearing samples from the "Série récurrente" have been collected in borehole 750/35 NE drilled horizontally at the –750 m mine level and from exposures in mine workings. Phlogopite and chlorite have been studied in the three types of ore mentioned above. They have been collected throughout the orebody from drill cores and outcrops in the mine. In the "Série récurrente", phlogopite and chlorite form a minor (2%) part of two mineral associations: (i) phlogopite, chlorite, dolomite and quartz forming pods in shale; and (ii) phlogopite, talc, albite, magnesite, dolomite,

TABLE 2. REPRESENTATIVE ELECTRON-MICROPROBE DATA ON PHLOGOPITE

Sample	11507		7502002		7502350	9921816		E3		KH102
SiO_2 wt.%	39.41	38.28	40.58	39.39	43.50	41.13	40.82	44.31	43.99	44.27
Al_2O_3	14.89	14.90	15.31	16.25	15.39	15.26	15.48	13.05	12.77	12.92
TiO_2	0.92	0.77	1.03	0.93	0.35	0.59	0.79	0.12	0.15	0.07
MnO	-	-	-	-	0.04	0.03	0.07	-	-	-
CuO	-	-	-	-	0.11	nd	nd	0.08	-	-
ZnO	n.d.	n.d.	-	-	-	0.13	0.04	n.d.	-	-
FeO	11.30	11.52	8.34	8.21	0.85	9.39	8.63	0.16	0.24	0.11
MgO	18.29	19.48	18.98	20.79	26.07	19.11	18.51	25.41	25.46	26.66
CaO	0.03	0.01	0.01	0.01	0.05	0.04	-	-	0.01	
BaO	-	-	-	-	-	0.08	0.26	0.18	0.37	0.13
Na_2O	0.13	0.07	0.06	0.03	0.06	0.14	0.11	0.14	0.16	0.08
K_2O	9.81	8.35	9.72	7.74	9.76	9.01	8.76	9.67	9.59	9.87
F	-	0.33	0.17	0.83	1.78	1.24	2.49	4.94	6.39	5.58
H_2O	4.08	3.88	4.04	3.69	3.44	3.57	2.94	1.92	1.20	1.86
F=O	-	-0.14	-0.07	-0.39	-0.75	-0.52	-1.05	-2.08	-2.69	-2.35
Total	98.86	97.43	98.16	97.59	98.81	99.29	97.97	97.90	97.63	99.01
	Formulas based on 24 (O, OH, F)									
Si	5.79	5.69	5.80	5.71	6.09	5.93	5.95	6.24	6.23	6.17
^{IV}Al	2.21	2.31	2.10	2.29	1.91	2.07	2.05	1.76	1.77	1.83
^{VI}Al	0.37	0.30	0.52	0.49	0.30	0.52	0.61	0.40	0.36	0.29
Ti	0.10	0.09	0.11	0.10	0.04	0.06	0.09	0.01	0.02	0.01
Fe	1.39	1.43	1.01	1.00	0.10	1.13	1.05	0.02	0.03	0.01
Mg	4.01	4.31	4.11	4.49	5.44	4.11	4.02	5.33	5.37	5.54
Mn	-	-	-	-	-	-	0.01	-	n.d.	n.d.
Zn	n.d.	n.d.	-	-	-	0.01	n.d.	n.d.	-	-
Cu	-	-	-	-	0.01	-	-	0.01	-	-
Σ	5.87	6.18	5.75	6.08	5.89	5.78	5.78	5.77	5.78	5.85
Ca	-	-	-	-	-	-	0.01	-	-	-
Ba	-	-	-	-	-	-	0.02	0.01	0.02	0.01
Na	0.04	0.02	0.02	0.01	0.02	0.04	-	0.04	0.04	0.02
K	1.84	1.58	1.80	1.43	1.74	1.66	1.63	1.74	1.73	1.76
Σ	1.88	1.60	1.82	1.44	1.76	1.70	1.66	1.79	1.79	1.78
F	-	0.15	0.08	0.43	0.79	0.56	1.15	2.20	2.86	2.46
OH	4.00	3.85	3.92	3.57	3.21	3.44	2.85	1.80	1.14	1.54

n.d.: not determined. A dash represents concentrations less than the detection limit of the electron microprobe and less than 0.001 atoms per formula unit. The proportion of H_2O was calculated.

TABLE 3. REPRESENTATIVE ELECTRON-MICROPROBE DATA ON CHLORITE

Sample	7502002		9921816		8112	8114		8116	
SiO_2 wt.%	29.62	30.45	28.28	28.86	27.72	25.95	26.68	26.23	26.29
Al_2O_3	21.79	20.45	22.36	22.67	21.53	19.82	19.20	19.74	19.48
TiO_2	0.05	-	-	0.04	-	0.02	0.01	0.07	-
MnO	0.04	-	0.05	0.03	-	0.05	0.15	0.07	-
CuO	-	-	n.d.	n.d.	n.d.	0.06	0.09	n.d.	n.d.
ZnO	n.d.	n.d.	0.25	-	-	n.d.	n.d.	-	0.64
FeO	9.54	9.68	13.48	13.03	13.23	32.02	32.43	32.41	34.31
MgO	25.79	27.05	22.77	22.89	23.79	9.71	9.33	10.01	9.23
CaO	-	0.03	0.02	0.09	0.01	0.03	-	-	0.05
BaO	-	1.39	0.03	-	0.14	-	-	-	-
Na_2O	0.03	0.14	0.02	0.02	-	0.03	-	0.03	-
K_2O	0.06	0.05	0.06	-	0.05	-	-	-	-
F	-	0.73	0.44	0.23	0.85	0.19	0.21	-	0.16
H_2O	12.37	12.18	11.93	12.17	11.89	10.91	10.91	11.10	11.06
F=O	-	-0.31	-0.19	-0.10	-0.27	-0.08	-0.09	-	-0.07
Total	99.29	101.83	99.55	100.21	99.95	98.71	98.92	99.70	101.17
	Formulas based on 16 (O, OH, F)								
Si	5.75	5.83	5.59	5.66	5.63	5.66	5.81	5.67	5.66
Al	4.98	4.62	5.21	5.22	5.04	5.10	4.93	5.03	4.95
Ti	0.01	-	-	0.01	-	-	-	0.01	-
Fe	1.55	1.55	2.23	2.13	2.18	5.84	5.91	5.85	6.18
Mg	7.46	7.72	8.71	8.66	8.97	3.16	3.30	3.22	2.96
Mn	0.01	-	0.01	0.01	-	0.01	-	0.01	-
Cu	-	-	-	-	-	0.01	0.01	-	-
Zn	n.d.	-	0.04	-	0.01	n.d.	n.d.	-	0.10
Ca	-	0.01	-	0.02	-	0.01	-	-	0.01
Ba	-	0.11	-	-	0.01	-	-	-	-
Na	0.01	0.05	0.01	0.01	-	0.01	-	0.01	-
K	0.01	0.01	0.02	-	0.01	-	-	-	-
F	-	0.44	0.28	0.14	0.40	0.13	0.14	-	0.11
OH	16.00	15.56	15.72	15.86	15.60	15.87	15.86	16.00	15.89
X_{Mg}	0.83	0.82	0.75	0.76	0.76	0.35	0.36	0.36	0.32

n.d.: not determined. A dash represents concentrations less than the limit of detection of the electron microprobe, i.e., and less than 0.001 atoms per formula unit. The proportion of H_2O was calculated.

gypsum, anhydrite and quartz in dolomite at the upper part of this unit. In this latter paragenesis, phlogopite is very sparse, and occurs as fine-grained, ragged flakes, whereas gypsum and anhydrite tend to form distinctive bands parallel to bedding.

In gabbro blocks, phlogopite and chlorite are associated with albite, amphibole (mostly tremolite and hornblende), epidote, quartz and calcite. Trace amounts (less than 1%) of disseminated chalcopyrite, pyrite and ilmenite also were observed. Albite, phlogopite and amphibole range in habit from fine-grained aggregates to very coarse grains intimately intergrown. Other components, such as epidote and quartz, commonly are limited to interstitial spaces. In some samples, albite porphyroblasts include small grains of epidote and phlogopite. Most of the chlorite seems to have developed as a product of alteration of phlogopite and amphibole, and was not analyzed.

Within the mineralized samples, phlogopite and chlorite occur in the following assemblages: (i) phlogopite, chlorite, muscovite, albite, quartz, dolomite, sphalerite, pyrite, galena, linnaeite, and (ii) phlogopite, chlorite, dolomite, quartz, albite, chalcopyrite, bornite, and minor arsenopyrite and sphalerite. Phlogopite grains embedded in sphalerite commonly are corroded by the sulfide.

Fluorite is very rare in the Kipushi deposit, and was not observed in this study; Intiomale & Oosterbosch (1974) reported its occurrence as disseminated grains on the –170 m and –850 m levels in the mine.

Mineral Compositions

Analyses of phlogopite and chlorite from different environments of the Kipushi deposit (Appendix 1) were performed on a Camebax Microbeam electron microprobe at the Université Pierre et Marie Curie, Paris VI, using an accelerating voltage of 15 kV, a beam current of 20 nA, and a counting time of 15 seconds. Standards used include orthoclase, diopside, albite, iron oxide, Mn and Ti oxide, sphalerite, fluorite and synthetic LiF. Results are listed in Tables 2 and 3 for phlogopite and chlorite, respectively.

Phlogopite

Figure 3 is a plot of analytical results on the biotite quadrilateral delimited by annite, phlogopite, aluminous annite, and aluminous phlogopite (Guidotti 1984).

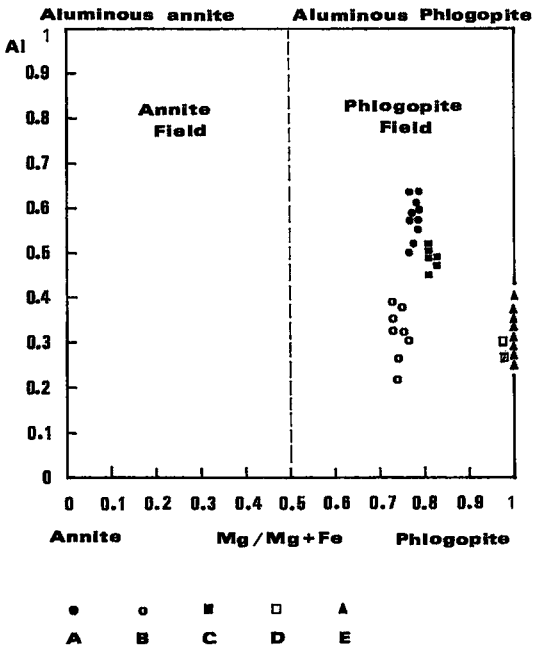

FIG. 3. Location of phlogopite from the Kipushi deposit in the phlogopite field of the biotite plane. Letters refer to: A: low F-bearing phlogopite associated with chalcopyrite (sample 9921816), B: phlogopite from gabbroic blocks (sample 11507), C: phlogopite found in barren shale of the "Série récurrente" (sample 7502002), D: phlogopite from gypsum-, anhydrite- and talc-bearing dolomite of barren "Upper Série récurrente" (sample 7502351), E: F-rich phlogopite from mineralized zones, associated both with sphalerite and chalcopyrite (samples E3 and KH 102).

It should be noted that aluminous annite and aluminous phlogopite are equivalent to the terms "siderophyllite" and "eastonite", respectively, used in the older literature (Deer *et al.* 1962). All the mica samples discussed in this paper plot in the compositional field of phlogopite.

Table 2 and Figure 3 indicate systematic variations in composition of phlogopite present in the various assemblages, which accordingly has been classified into five categories (A – E), as explained in the caption to Figure 3. Ore-related phlogopite associated with sphalerite as the dominant sulfide mineral exhibits a very high F content, ranging from 4.41 to 6.39 wt.% F (category E). These phlogopite samples are distinctly more Mg-rich than those from barren rocks and plot on the phlogopite – aluminous phlogopite join. Their X_{Mg} value [where X_{Mg} = Mg/(Mg + Fe)] approaches unity (more than 0.99). Phlogopite associated with chalcopyrite as the dominant sulfide mineral shows a greater spread in F content, ranging from 1.24 to 5.35 wt.% F, whereas their X_{Mg} varies from 0.77 to more than 0.99 for the material richest in F (which is included in category E). These fluorine contents are comparable to those found by Gunow *et al.* (1980) in biotite from the Henderson molybdenite deposit, Colorado. The mol fraction of the phlogopite end-member (X_{phl} = Mg/total octahedrally coordinated cations) in ore-related phlogopite extends from 0.68 to 0.71 for relatively F-poor compositions associated with chalcopyrite as the dominant sulfide mineral (category A) and from 0.92 to 0.95 for F-rich phlogopite from both sphalerite and chalcopyrite ores (category E). Phlogopite found in the metamorphosed Luisha copper deposit 45 km NNW of Kipushi displays similar values of X_{Mg} (Cluzel 1986).

Phlogopite from barren shale of the "Série récurrente" (category C) and from barren gabbro blocks (category B) is characterized by the lowest concentrations of F, ranging from 0 to 1.0 wt.% F. These samples of phlogopite have X_{Mg} values varying from 0.81 to 0.83 and from 0.73 to 0.76, corresponding to X_{phl} values ranging from 0.71 to 0.74 and from 0.67 to 0.71, respectively. Phlogopite from barren dolomite of the Upper "Série récurrente", coexisting with talc, magnesite, gypsum and anhydrite (category D) has a low F content like that in phlogopite from barren gabbro and shale, but its X_{phl} is in the range of those of the F-rich phlogopite described above.

The above relations are illustrated in Figure 4. Excluding the phlogopite of category D, fluorine abundances and X_{phl} vary sympathetically, a feature that has been reported by several other investigators (*e.g.*, Zaw & Clark 1978, Jacobs & Parry 1979, Munoz 1984, 1992). This is an expression of the Fe–F avoidance rule (Mason 1992, Zhu & Sverjensky 1992).

Among the various mineral assemblages, fluorine exhibits its most pronounced correlation with X_{phl} in the phlogopite from barren environments (phlogopite

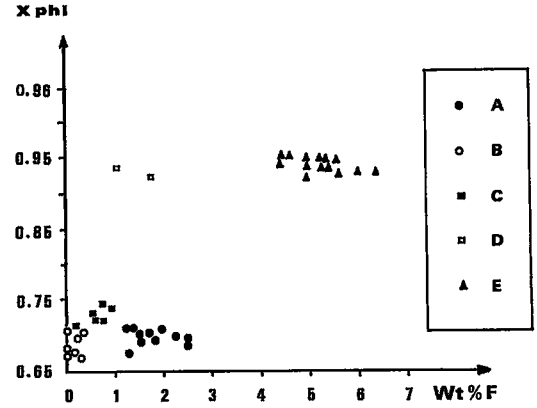

FIG. 4. Plot of concentration of *F versus* X_{phl}, defined as the ratio Mg/total octahedrally coordinated cations.

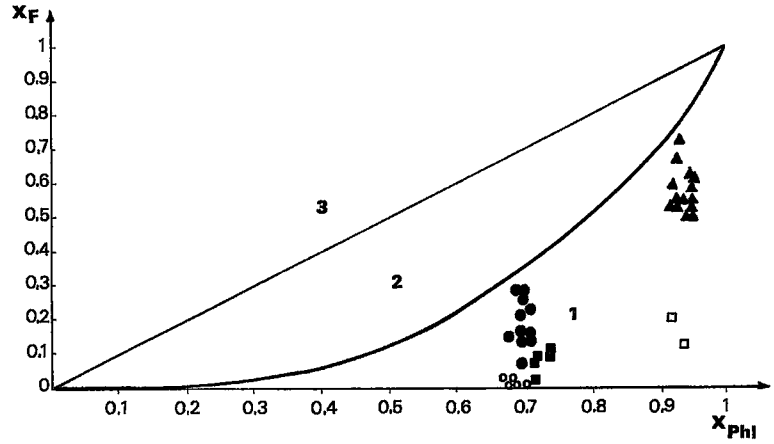

FIG. 5. Location of the phlogopite from Kipushi in $X_{phl} - X_F$ space. 1: Field of disordered distribution of octahedrally coordinated cations. 2: Field of cluster formation. 3: Field in which the Fe–F avoidance rule is violated. Modified after Mason (1992). Symbols as in Fig. 3.

of categories B and C). F-rich phlogopite from the mineralized samples (category E) displays a tendency for an unusual, albeit weak, inverse relationship between these compositional variables. Although this observation seems to be a violation of the Fe–F avoidance rule, it probably indicate that the phlogopite equilibrated with fluids of different compositions (Zhu & Sverjensky 1992).

When plotted in X_F and X_{phl} space (Fig. 5), all the compositions of phlogopite from the Kipushi deposit fall in the field characterized by Fe–F avoidance and a random (disordered) distribution of octahedrally coordinated cations (Mason 1992), indicating that the maximum mol fraction of F that could be accommodated has not been attained, and that no Mg–F and Fe–OH clusters occur.

In general, phlogopite with a high X_{phl} value has a high Si content and a low Ti content (Fig. 6). Guidotti *et al.* (1977) and Guidotti (1984) also have reported an antipathy between Si and Ti in biotite with high Mg/(Mg + Fe) values. In some mineral assemblages, these relations are very poorly defined; in others, an opposite relationship is found, particularly in ore-related, F-rich (category E) phlogopite (Fig. 7). In the phlogopite from Kipushi, the $^{IV}Al/Si$ ratio is less than 1:3. Octahedrally coordinated Al shows a negative correlation with X_{phl} (Fig. 8), as noted by Valley *et al.* (1982) and Munoz (1984). In this respect, ^{VI}Al has the same influence on F–OH exchange in biotite as Fe^{2+} (Zhu & Sverjensky 1991, 1992). The variation in X_{Mg} values of phlogopite from the Kipushi deposit is comparable to that observed in metamorphosed deposits (*e.g.*, Nesbitt & Kelly 1980, Nesbitt 1982, 1986b).

Phlogopite also is characterized by significant amounts of Ti, which is enriched in F-poor micas from the barren "Série récurrente" and gabbro, as mentioned above. Barium commonly is present, but rarely exceeds 0.40 wt.% BaO. This contrasts with the considerable amounts of Ba (up to 7.86 wt.% BaO) found in muscovite of this deposit (Chabu & Boulègue 1992). The occupancy of the 12-coordinated sites is relatively low, varying from 1.44 to 1.94 atoms per formula unit (apfu). Guidotti (1984) noted that an inverse relationship exists between very high X_{Mg} and total 12-coordinated cations. However, the plot of these compositional parameters shows considerable scatter, casting doubt on the existence of the above relation in the mica analyzed.

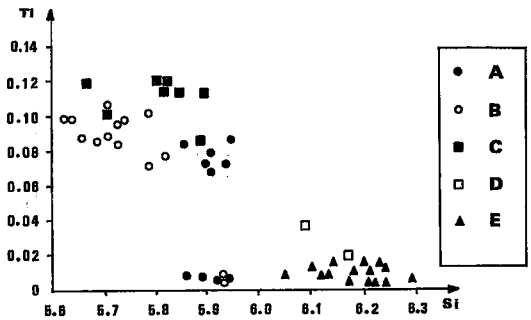

FIG. 6. Relationship between Ti and Si. Symbols as in Fig. 3.

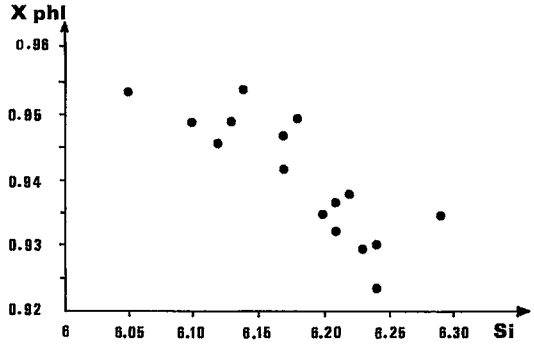

FIG. 7. Relationship between X_{phl} and Si contents of ore-related, F-rich phlogopite (category E).

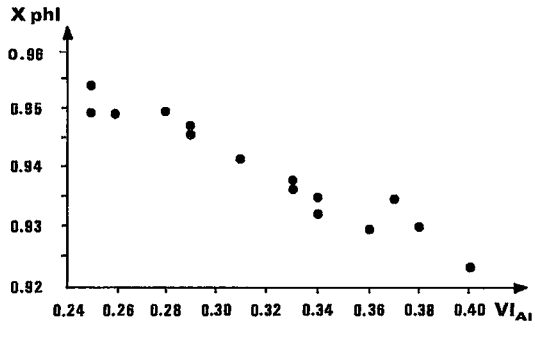

FIG. 8. Plot of proportion of octahedrally coordinated Al *versus* X_{phl} of ore-related phlogopite.

Chlorite

Chlorite has very low F content (0 to 0.73 wt.%) compared to the coexisting phlogopite. This confirms that F is preferably partitioned in the mica. Figure 9 and Table 3 show a considerable range in the composition of chlorite, with X_{Mg} values ranging from 0.32 to 0.84. Systematic relationships with respect to the ores exist: the chlorite associated with iron-rich sphalerite (up to 7.86 mol % FeS) as the dominant sulfide is the most Fe-rich ($0.32 < X_{Mg} < 0.76$); that associated with chalcopyrite ores is more Mg-rich ($X_{Mg} = 0.76$), whereas that found in unmineralized shale of the "Série récurrente" is the richest of all in Mg ($X_{Mg} = 0.83$, mean value). Similar trends in chlorite compositions have been observed in metamorphosed Cu-sulfide deposits (Bachinski 1976). They do not agree with compositional variations resulting from sulfidation reactions (Guidotti *et al.* 1991), and suggest that the Mg/(Mg + Fe) ratio of chlorite could depend on the Fe contents of the associated sphalerite.

Although no chlorite was observed in association with the most Mg-rich phlogopite, the chlorite compositions seem to vary in antipathy with those of phlogopite, which is more Mg-rich ($X_{Mg} > 0.99$) in ores than in the host rocks, in agreement with theoretical considerations on sulfidation reactions (Thompson 1976a, b, Nesbitt 1986a, Guidotti *et al.* 1988, 1991) and with observations made in metamorphosed sulfide deposits (Koo & Mossman 1975,

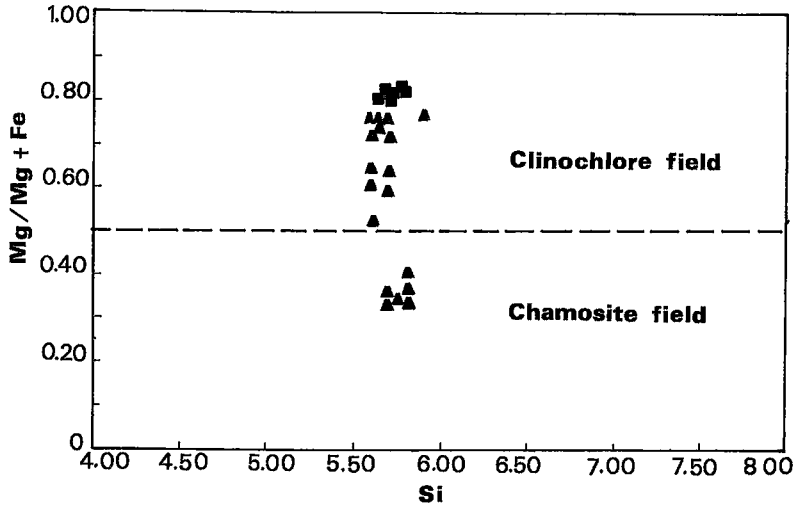

FIG. 9. Chemical composition of chlorite from the Kipushi deposit. Symbols as in Fig. 3. See also Table 3 and Appendix 1.

Nesbitt & Kelly 1980, Nesbitt 1982, 1986b).

Despite the absence of any textural evidence, the reversed pattern of the chlorite composition compared to that of phlogopite may indicate that the chlorite associated with sphalerite is secondary in origin. However, Tewhey & Hess (1975) and Guidotti *et al.* (1975) have shown that the Mg/Fe ratio of chlorite and biotite are reversed in extremely Mg-enriched rocks. This could possibly apply to the dolomitic rocks that host the Kipushi deposit.

Where coexisting, phlogopite and chlorite have similar X_{Mg} values, although the value of chlorite commonly is slightly higher by 0.02. This indicates that chemical equilibrium may have been attained between these minerals, which would cast doubt on the secondary nature of the chlorite mentioned above.

The Si and Al_{total} contents of chlorite are relatively constant in all the mineral assemblages. This has also been observed by Guidotti *et al.* (1991).

TABLE 4. F/OH EXCHANGE EQUILIBRIUM CONSTANTS

	A	B	C	D	E
Molar proportions					
X_{phl}	0.70(0.01)	0.70(0.02)	0.73(0.01)	0.93(0.01)	0.94(0.01)
X_F	0.20(0.05)	0.02(0.014)	0.07(0.03)	0.16(0.06)	0.58(0.06)
X_{OH}	0.80(0.05)	0.98(0.014)	0.93(0.03)	0.84(0.06)	0.42(0.06)
Temp.			log(f(H_2O)/f(HF)) in fluid		
250°C	7.04	8.13	7.61	7.64	6.80
300°C	6.52	7.60	7.08	7.08	6.24
350°C	6.08	7.16	6.63	6.60	5.76
400°C	5.70	6.79	6.25	6.20	5.35

Values in parentheses represent one standard deviation. Labels (letters A, B, C, D and E) correspond to different mineral assemblages (see Fig. 3). A: average result of 19 analyses; B: average result of 8 analyses; C: average result of 8 analyses; D: average result of 2 analyses; E: average result of 16 analyses. Only analyses of F-bearing phlogopite have been included in the calculations. Molar proportions were determined according to the following equations: $X_{phl} = X_{phlogopite}$ = Mg/total octahedrally coordinated cations; X_F = F atoms per formula unit/4; X_{OH} = OH content per formula unit/4.

F–OH Exchange Equilibria

A generalized reaction for F–OH exchange of biotite with a fluid can be written as follows (*e.g.*, Gunow *et al.* 1980, Parry *et al.* 1984):

OH(mica) + HF(fluid) = F(mica) + H_2O(fluid);

the equilibrium constant is

$\log K = \log(X_F/X_{OH})$ mica + $\log[f(H_2O)/f(HF)]$ fluid.

Theoretical considerations and experimental data (Munoz & Ludington 1974, Gunow *et al.* 1980, Valley & Essene 1980, Valley *et al.* 1982, Munoz 1984, Zhu & Sverjensky 1991) on OH–F partitioning between a mica and a fluid phase have established that the F/OH ratio of biotite is dependent on (i) the fugacity ratio $f(H_2O)/f(HF)$ of the fluid, (ii) temperature, and (iii) the cation population of the octahedral sites.

Calculations of $\log[f(H_2O)/f(HF)]$ at temperatures varying from 250 to 400°C were made using equation

$\log[f(H_2O)/f(HF)]$ in fluid =

$$1/T(2371 + 1100X_{Mg}) + 0.433 - \log(X_F/X_{OH})$$

as discussed by Munoz (1992). Results are shown in Table 4.

Temperature may be inferred from observed assemblages of metamorphic minerals: (i) dolomite, albite, muscovite, quartz, phlogopite and chlorite in ores, (ii) dolomite, quartz, albite, talc, magnesite, phlogopite in gypsum and anhydrite-bearing dolomite, and (iii) phlogopite, chlorite, quartz in shales of the "Série récurrente" above the mineralization. These mineral assemblages support the suggestion by Lefebvre & Patterson (1982) that the Kipushi deposit is located in the biotite zone of the regional metamorphism.

Available experimental data (Winkler 1965, 1967, Puhan & Johannes 1974) and studies of metamorphosed carbonate rocks (Pinsent & Smith 1975, Ferry 1976, Rice 1977, Bowman & Essene 1982) are consistent with the first development of biotite, under a water pressure of a few kilobars, at temperature between 300 and 400°C. The biotite–chlorite isograd reaction muscovite + dolomite + quartz + water = biotite + chlorite + calcite + carbon dioxide, which seems to apply to the mineral assemblages found in the Kipushi deposit, was estimated to occur at 370°C in the metamorphism of impure dolomite (Ferry 1976).

Experimental data (Fawcett & Yoder 1966) indicate that magnesium-rich chlorite is stable in a wider range of P–T conditions than Fe-rich chlorite. The stability field of the latter is drastically limited under reducing conditions at a temperature above 350°C under a

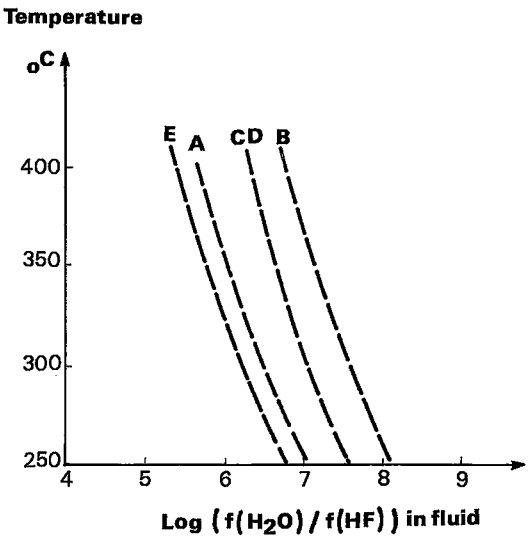

FIG. 10. Log $[f(H_2O)/f(HF)]$ contours defining the fluid phase coexisting with phlogopite of different fluorine contents involved in the five mineral assemblages described in Fig. 3. Labeling as in Fig. 3.

pressure of 1 kbar. Since Fe-bearing chlorite is present in the reducing environment of the Kipushi ores, it is reasonable to assume that the temperature that affected the deposit during the Katangan regional metamorphism was below 350°C. The amount of ^{IV}Al in the chlorite (half formula) suggests that this mineral formed at a temperature varying from 287 to 331°C (Cathelineau & Nieva 1985, Cathelineau 1988). This is in agreement with Cluzel's (1986) estimate of the P–T conditions of the Katangan regional metamorphism in the area.

Given these limiting conditions, it is assumed that F–OH exchange reactions took place at temperatures between 300 and 350°C. Variations of $\log[f(H_2O)/f(HF)]$ both within and between different mineral associations are shown in Figure 10. This indicates that at any temperature, the relative activity of HF is higher in ores (curves A and E) than in barren rocks (curves B, C and D). The variation in log fugacity ratio within the ores indicates that the composition of the fluids with which the mica equilibrated varied significantly.

Conclusions

The data presented in this paper clearly indicate that the composition of phlogopite and chlorite is a function of mineral assemblage and that chemical equilibrium has been attained among the different phases of each association.

Earlier, it was noted that the X_{Mg} of phlogopite varies sympathetically with Si and that Ti decreases with increasing Si. This compositional variation is obviously controlled by crystallochemical factors and involves a Tschermak exchange $(Mg, Fe^{2+}) + Si = {}^{VI}Al + {}^{IV}Al$, and possibly also the scheme $2(Mg, Fe^{2+}) = {}^{IV}Ti + {}^{VI}\square$ (Guidotti 1984).

The pattern of variation in X_{Mg} in phlogopite agrees with a control exerted by sulfidation reactions, whereas the compositional variation found in chlorite, although similar to that observed by Bachinski (1976) in metamorphosed cupriferous iron deposits, is unexpected as far as sulfidation reactions are concerned (Guidotti *et al.* 1991). The data seem to suggest that the Fe content of chlorite depends on the concentration of iron in the coexisting sphalerite.

The relationship between X_{phl} and F concentration in phlogopite is compatible with the existence of a field of Fe–F avoidance in the compositional field of biotite. Despite its very high levels, F is not at its saturation level in phlogopite owing to the high X_{Mg} values of the mica.

That the fluorine contents of the fluids with which phlogopite equilibrated within the Kipushi mineralized samples were high is shown both by the extremely high concentrations of fluorine in mica and by the correspondingly low calculated log fugacity ratios.

The generation of phlogopite and chlorite in ores may be ascribed to ore-forming processes or to metamorphic processes. The second hypothesis is preferred because of the presence of similar assemblages of metamorphic minerals beyond the zone of mineralization, occurring on a regional scale from the Zambian segment of the Copperbelt to the Kipushi area and through to the Musoshi area (Lefebvre & Patterson 1982). Moreover, widespread structural and textural features relatable to the Katangan regional metamorphism indicate that the deposit is premetamorphic in age (Chabu 1990, Chabu & Boulègue 1992). This is supported by the variations in X_{Mg} values of phlogopite, which can be attributed to increasing $f(F)$ and $f(S_2)$ toward the orebody during the metamorphism of the deposit (Hutcheon 1979, Nesbitt 1986a, b).

Investigations of metamorphic paragenesis have shown that the fluorine content of hydrous minerals depends directly upon the amount of fluorine present in the premetamorphic protolith (Valley *et al.* 1982, Guidotti 1984). This fact suggests that fluorine in phlogopite was inherited from the breakdown, during the Lufilian metamorphism, of fluorite or some other F-rich precursor present in the sulfide assemblages. Variation in F contents of phlogopite reflects an inhomogeneous distribution of fluorine-rich minerals in the ores prior to regional metamorphism, resulting in variable F/OH activities in the metamorphic fluids.

The composition of the phlogopite and chlorite is thus a function of mineral assemblages, oxygen, sulfur and HF activities. Taken in conjunction with regional metamorphic setting, they provide additional evidence that the mineralization predated the Lufilian folding and metamorphism.

Acknowledgements

The manuscript has benefitted considerably from comments, suggestions and criticism by Drs. J.L. Munoz, C.V. Guidotti, R.A. Mason and R.F. Martin. Sincere thanks are also due to the Laboratoire de Géochimie et Métallogénie, Université Paris VI, for technical, analytical and scientific assistance.

References

Bachinski, D.J. (1976): Metamorphism of cupriferous iron sulfide deposits, Notre Dame Bay, Newfoundland. *Econ. Geol.* **71**, 443-452.

Bowman, J.R. & Essene, E.J. (1982): P–T–X(CO_2) conditions of contact metamorphism in the Black Butte aureole, Elkhorn, Montana. *Am. J. Sci.* **282**, 311-340.

Cathelineau, M. (1988): Cation site occupancy in chlorites and illites as a function of temperature. *Clay Minerals* **23**, 471-485.

_____ & Nieva, D. (1985): A chlorite solid solution geothermometer. The Los Azufres (Mexico) geothermal system. *Contrib. Mineral. Petrol.* **91**, 235-244.

CHABU, M. (1990): Metamorphism of the Kipushi carbonate hosted Zn–Pb–Cu deposit (Shaba, Zaire). *In* Regional Metamorphism of Ore Deposits and Genetic Implications (P.G. Spry & L.T. Bryndzia, eds.). VSP, Utrecht, Holland (27-47).

_____ & BOULÈGUE, J. (1992): Barian feldspar and muscovite from the Kipushi Zn–Pb–Cu deposit, Shaba, Zaire. *Can. Mineral.* **30**, 1143-1152.

CLUZEL, D. (1986): Contribution à l'étude du métamorphisme des gisements cupro-cobaltifères stratiformes du Sud-Shaba, Zaïre. Le district minier de Luisha. *J. Afr. Earth Sci.* **5**, 557-574.

DEER, W.A., HOWIE, R.A. & ZUSSMAN, J. (1962): *Rock-Forming Minerals.* **3**. *Sheet Silicates.* Longmans, London, U.K.

DE MAGNÉE, I. & FRANÇOIS, A. (1988): The origin of the Kipushi (Cu, Zn, Pb) deposit in direct relation with a Proterozoic salt diapir. Copperbelt of Central Africa, Shaba, Republic of Zaire, *In* Base Metal Sulfide Deposits (G.H. Friedrich & P.M. Herzig, eds.). Springer Verlag, Berlin, Germany (74-93).

FAWCETT, J. & YODER, H.S. (1966): Phase relationship of chlorites in the system $MgO–Al_2O_3–SiO_2–H_2O$. *Am. Mineral.* **51**, 353-380.

FERRY, J.M. (1976): Metamorphism of calcareous sediments in the Waterville–Vassalboro area, south central Maine: mineral reactions and graphical analysis. *Am. J. Sci.* **276**, 841-882.

GUIDOTTI, C.V. (1984): Micas in metamorphic rocks. *In* Micas (S.W. Bailey, ed.). *Rev. Mineral.* **13**, 357-467.

_____, CHENEY, J.T. & CONATORE, P.D. (1975): Coexisting cordierite + biotite + chlorite from Rumford Quadrangle, Maine. *Geology* **3**, 147-148.

_____, _____ & GUGGENHEIM, S.(1977): Distribution of titanium between coexisting muscovite and biotite in pelitic schists from northwestern Maine. *Am. Mineral.* **62**, 438-448.

_____, _____ & HENRY, D.J. (1988): Compositional variations of biotite as a function of metamorphic reactions and mineral assemblage in the pelitic schists of western Maine. *Am. J. Sci.* **288A**, 270-292.

_____, TEICHMANN, F. & HENRY, D.J. (1991): Chlorite-bearing polymetamorphic metapelites in the Rangeley area, Maine: evidence for equilibrium assemblages. *Am. Mineral.* **76**, 867-879.

GUNOW, A.J., LUDINGTON, S.D. & MUNOZ, J.L. (1980): Fluorine in micas from the Henderson molybdenite deposit, Colorado. *Econ. Geol.* **75**, 1127-1137.

HUTCHEON, I. (1979): Sulfide – oxide – silicate equilibria; Snow Lake, Manitoba. *Am. J. Sci.* **279**, 643-665.

INTIOMALE, M.M. (1982): *Le gisement Zn–Pb–Cu de Kipushi (Shaba, Zaïre). Etudes géologique et métallogénique.* Thèse de doctorat, Univ. Catholique de Louvain, Louvain-la-Neuve, Belgique.

_____ & OOSTERBOSCH, R. (1974): Géologie et géochimie du gisement de Kipushi, Zaïre. *In* Gisements stratiformes et provinces cuprifères (P. Bartholomé, ed.). Société Géologique de Belgique, Liège, Belgique (123-164).

JACOBS, D.C. & PARRY, W.T. (1979): Geochemistry of biotite in the Santa Rita porphyry copper deposit, New Mexico. *Econ. Geol.* **74**, 860-887.

KOO, J. & MOSSMAN, D.J. (1975): Origin and metamorphism of the Flin Flon stratabound Cu–Zn sulfide deposit, Saskatchewan and Manitoba. *Econ. Geol.* **70**, 48-62.

LEFEBVRE, J.J. (1975): Les roches ignées dans le Katangien du Shaba, Zaïre, le district du cuivre. *Soc. Géol. Belg., Annales* **98**, 47-73.

_____ & PATTERSON, L.E. (1982): Hydrothermal assemblage of aluminian serpentine, florencite and kyanite in the Zairian Copperbelt. *Soc. Géol. Belg., Annales* **105**, 51-71.

MASON, R.A. (1992): Models of order and iron–fluorine avoidance in biotite. *Can. Mineral.* **30**, 343-354.

MUNOZ, J. L. (1984): F–OH and Cl–OH exchange in micas with applications to hydrothermal ore deposits. *In* Micas (S.W. Bailey, ed.). *Rev. Mineral.* **13**, 469-493.

_____ (1992): Calculations of HF and HCl fugacities from biotite compositions: revised equations. *Geol. Soc. Am., Abstr. Programs* **24**, A221.

_____ & LUDINGTON, S.D. (1974): Fluoride–hydroxyl exchange in biotite. *Am. J. Sci.* **274**, 396-413.

_____ & _____ (1977): Fluorine–hydroxyl exchange in synthetic muscovite and its application to muscovite–biotite assemblages. *Am. Mineral.* **62**, 304-308.

NESBITT, B.E. (1982): Metamorphic sulfide–silicate equilibria in the massive sulfide deposits at Ducktown, Tennessee. *Econ. Geol.* **77**, 364-378.

_____ (1986a): Oxide – sulfide – silicate equilibria associated with metamorphosed ore deposits. I. Theoretical considerations. *Econ. Geol.* **81**, 831-840.

_____ (1986b): Oxide – sulfide – silicate equilibria associated with metamorphosed ore deposits. II. Pelitic and felsic volcanic terrains. *Econ. Geol.* **81**, 841-856.

_____ & KELLY, W.C. (1980): Metamorphic zonation of sulfides, oxides and graphite in and around the orebodies at Ducktown, Tennessee. *Econ. Geol.* **75**, 1010-1021.

PARRY, W.T., BALLANTYNE, J.M. & JACOBS, D.C. (1984): Geochemistry of hydrothermal sericite from Roosevelt Hot Spring and the Tintic and Santa Rita porphyry copper system. *Econ. Geol.* **79**, 72-86.

PINSENT, R. & SMITH, D.G.W. (1975): The development of carbonate bearing biotite isograd assemblages from Tete Jaune Cache, British Colombia, Canada. *Can. Mineral.* **13**, 151-161.

PUHAN, D. & JOHANNES, W. (1974): Experimentelle Undersuchung der Reaktion Dolomit + Kalifeldspat + H_2O = Phlogopit + Calcit + CO_2. *Contrib. Mineral. Petrol.* **48**, 23-31.

RICE, J.M. (1977): Progressive metamorphism of impure dolomitic limestone in the Marysville aureole, Montana. *Am. J. Sci.* **277**, 1-24.

TEWHEY, J.D. & HESS, P.C. (1975): Continuous metamorphic facies changes as related to chlorite disappearance in a contact metamorphic aureole. *Geol. Soc. Am., Abstr. Programs* **7**, 80.

THOMPSON, A.B. (1976a): Mineral reactions in pelitic rocks. I. Predictions of P–T–X(Fe–Mg) phase relations. *Am. J. Sci.* **276**, 401-424.

_____ (1976b): Mineral reactions in pelitic rocks. II. Calculations of some P–T–X(Fe–Mg) phase relations. *Am. J. Sci.* **276**, 425-454.

UNRUG, R. (1988): Mineralization controls and source of metals in the Lufilian fold belt, Shaba (Zaire), Zambia and Angola. *Econ. Geol.* **83**, 1247-1258.

VALLEY, J.W. & ESSENE, E.J. (1980): Calc-silicate reactions in Adirondack marbles: the role of fluids and solid solutions: summary (parts I and II). *Geol. Soc. Am., Bull.* **91**, 114-117, 720-815.

_____, PETERSEN, E.U., ESSENE, E.J. & BOWMAN, J.R. (1982): Fluorphlogopite and fluortremolite in Adirondack marbles and calculated C–O–H–F compositions. *Am. Mineral.* **67**, 545-557.

WINKLER, H.G.F. (1965): *La genèse de roches métamorphiques.* Springer Verlag, Berlin, Allemagne.

_____ (1967): *Petrogenesis of Metamorphic Rocks* (second edition). Springer Verlag, Berlin, Germany.

ZAW, U.K. & CLARK, A.H. (1978): Fluoride–hydroxyl ratios of skarn silicates, Cantung E-zone scheelite orebody, Tungsten, Northwest Territories. *Can. Mineral.* **16**, 207-221.

ZHU, CHEN & SVERJENSKY, D.A. (1991): Partitioning of F–Cl–OH between minerals and hydrothermal fluids. *Geochim. Cosmochim. Acta* **55**, 1837-1858.

_____ & _____ (1992): F–Cl–OH partitioning between biotite and apatite. *Geochim. Cosmochim. Acta* **56**, 3435-3467.

Received August 23, 1993, revised manuscript accepted October 25, 1994.

APPENDIX 1. MINERAL ASSEMBLAGES IN THE SAMPLES ANALYZED

Sample	Rock description
11507	Gabbro fragment of the axial zone of the Kipushi breccia. Composition: phlogopite, albite, tremolite, hornblende, chlorite, quartz, epidote and minor hematite, rutile, chalcopyrite, calcite. Barren.
7502002	Barren shale of the upper part of the "Série récurrente". It is composed of sericite and fine-grained chlorite and quartz. Pods of coarse-grained phlogopite, quartz, dolomite and chlorite are scattered in the groundmass. Only these coarse grains were analyzed.
7502351	Grey dolomite from the upper part of the "Série récurrente". Composition: dolomite, talc, albite, magnesite, quartz, phlogopite, with lenses of gypsum and anhydrite. Barren.
9921816	Ore sample. Mineralized breccia composed of fragments of shale and dolomite. Dolomite, sulfide minerals and accessory quartz form the matrix. Chalcopyrite is the dominant sulfide; arsenopyrite and sphalerite are present. Phlogopite and chlorite are located in the matrix and are intergrown with chalcopyrite. Phlogopite is corroded by chalcopyrite, dolomite and quartz.
E3	Ore sample. Breccia composed of debris of Upper Kakontwe carbonaceous dolomite and fragments of shale of the "Série récurrente", cemented by Fe-poor sphalerite, which includes pyrite, arsenopyrite, chalcopyrite, galena, tennantite and bornite grains. Phlogopite is embedded in sphalerite and is strongly corroded by it. Neoformed muscovite is present both in dolomite and shale fragments. Coarse-grained quartz and dolomite are also present in the matrix.
KH 102	Mineralized sample. The rock is a medium- to coarse-grained dolomite with small layer of shale, displaying a microfold. It is mineralized both in the groundmass and in fissures. Chalcopyrite is the dominant sulfide mineral, whereas pyrite, arsenopyrite and bornite are minor. Phlogopite is intergrown with chalcopyrite, dolomite and quartz and form radiating flakes in veins.
8112	Mineralized breccia. The fragments are derived from a fine-grained sandstone (the "lambeau", see text) and shale of the "Série récurrente". The matrix is mostly composed of Fe-rich sphalerite and quartz. Chlorite and muscovite also are present.
8114	Ore sample. The major constituents of this mineralized breccia are fragments of shale that contain oriented sericite. The interfragmental voids are filled by brown Fe-enriched sphalerite, quartz, muscovite, chlorite, albite, dolomite.
8116	This sample has a modal composition similar to that of the preceding sample (8114).